Effect of Chelation Chemistry of Sodium Polyaspartate on the Dissolution of Calcite

You-Ting Wu and Christine Grant*

Department of Chemical Engineering, Campus Box 7905, North Carolina State University, Raleigh, North Carolina 27695-7905

Received December 21, 2001. In Final Form: April 17, 2002

Polyaspartic acid (PASP) is an environmentally benign agent for the dissolution of calcium salt deposits. In this study, the chelating power of PASP with calcium is investigated by performing the potentiometric titration against PASP solutions. It was found that PASP is fully deprotonated at pH 7. The titration curves are successfully modeled by assuming that four aspartyl residues from an actual PASP molecule consist of a hypothetical molecule (denoted as H_4L) that has four distinct acid moieties (four dissociation constants). The resulting dissociation constants and calcium-binding constants for PASP are critical to understanding the dissolution behavior of calcite in PASP solutions. The batch dissolution of calcite powder in PASP solution at four different initial pHs (10, 7, 5, and 3.5) are performed to explore the effect of PASP chelating chemistry on the dissolution behavior of calcite ($CaCO_3$). The results show that PASP replaces interfacial water to react with calcite at high pH ($\geq$7) and the dissolution of calcite can be described by a surface adsorption and complexation mechanism. At low pH ($\leq$5), surface adsorption of PASP on calcite surface still plays an important role, and both acidic species attacks (H^+ and H_nL^{n-4}, $n = 1,2,3,4$, attacking carbonate sites) and chelant attacks (L^{4-} and H_nL^{n-4}, $n = 1,2$, attacking calcium sites) affect the calcite dissolution. The dissolution of calcite in acidic PASP solutions represents the most complicated case.

1. Introduction

The dissolution of calcite is of interest for food and chemical industries. One of the most important chemical industrial problems associated with calcium salt deposition is the scaling of water cooling or heating systems. Due to the inverse solubility of calcium salts at higher temperatures, soluble calcium minerals tend to form sparingly soluble scales on the surfaces of heat exchangers and evaporators. Likewise, high-temperature (120−140 °C) daily processing of milk causes the formation of mineral-rich protein fouling deposits (containing 70 wt % calcium mineral).[1] The precipitation and deposition of these hardness minerals on industrial processing equipment lowers the efficiency of heat exchange surfaces and obstructs fluid flow in piping. The cleaning of these deposits from processing equipment becomes important. Since calcite (calcium carbonate) is one of the most important calcium mineral deposits, a fundamental understanding of the surface interactions of cleaning agents on calcite dissolution is required.

In general, several kinds of reagents can be used to dissolve calcium salt deposits. Most studies in the literature[2−9] use small-molecule inorganic acids such as hydrochloric acid, sulfuric acid, and acetic acid to dissolve calcium salts. This is because inorganic acids can provide H^+ in aqueous solution and calcite has a high solubility at low pHs. While low pHs favor dissolution, the use of strongly acidic solutions is impractical in many applications and undesirable in others, mainly due to the inherent toxicity and high levels of reactivity of strong acids. The toxicity and high levels of reactivity cause corrosion in metallic process equipment and piping systems, and harm the environment when discharging the solution. As alternatives, many calcium chelating agents[10−13] such as citrate, EDTA, and other aminopolycaboxylic acids, have been used to enhance calcium salt dissolution. However, EDTA and other aminopolycarboxylic acids usually degrade slowly in the environment and their strong chelating power has raised concerns about their role in heavy metal mobilization in groundwater.[14,15] Therefore, it is necessary to seek alternative environmentally benign chelating agents for the dissolution of calcite deposits.

Our research group has demonstrated the use of sodium polyaspartate (Na−PASP) for enhancing the removal rates of hydroxyapatite and brushite deposits from the surface of stainless steel under turbulent flow.[16] PASP is a promising polycarboxylic sequestrant that is nontoxic, highly biodegradable, and water soluble.[17] As shown in Figure 1, the sequestrant consists of polymerized α- and β-aspartyl residues, each containing a carboxylic functional group that can combine with H^+ or metal ions to form different H−PASP or metal−PASP species at dif-

(1) Burton, H. *J. Daily Res.* **1968**, *35*, 317−330.
(2) Nierode, D. E.; Williams, B. B. *Soc. Pet. Eng. J.* **1971**, *11* (4), 406−418.
(3) Berner, R. A.; Morse, J. W. *Am. J. Sci.* **1974**, *274*, 108−134.
(4) Lund, K.; Fogler, H. S.; McCune, C. C.; Ault, J. W. *Chem. Eng. Sci.* **1975**, *30*, 825−835.
(5) Plummer, L. N.; Wigley, T. M. L.; Parkhurst, D. L. *Am. J. Sci.* **1978**, *278*, 179−216.
(6) Sjoberg, E. L.; Rickard, D. T. *Chem. Geol.* **1984**, *42*, 119−136.
(7) Compton, R. G.; Daly, P. J. *J. Colloid Interface. Sci.* **1984**, *101* (1), 159−166.
(8) Fredd, C. N.; Fogler, H. S. *Chem. Eng. Sci.* **1998**, *53* (22), 3863−3874.
(9) Grant, C. S.; Webb, G.; Jeon, Y. *AIChE J.* **1996**, *42*, 861−875.
(10) Terabayashi, T.; Sawa, T.; Ueno, M. *Colloids Surf., B: Biointerfaces* **1996**, *7*, 249−257.
(11) Christoffersen, J.; Christoffersen, M. R.; Arends, J. *Croat. Chem. Acta* **1983**, *56*, 769−777.
(12) Arbel, A.; Katz, I.; Sarig, S. *J. Cryst. Growth* **1991**, *110*, 733.
(13) Fredd, C. N.; Fogler, H. S. *J. Colloid Interface Sci.* **1998**, *204*, 187−197.
(14) Means, J. L.; Kucak, T.; Crerar, D. A. *Environ. Pollut., Ser. B* **1980**, *1*, 45−60.
(15) Xue, H. B.; Sigg, L.; Kari, F. G. *Environ. Sci. Technol.* **1995**, *29*, 59−68.
(16) Littlejohn, F.; Saez, A. E.; Grant, C. S. *Ind. Eng. Chem. Res.* **1998**, *37*, 2691−2700.
(17) Freeman, M. B.; Paik, Y. H.; Wilczynski, R.; Wolks, S. K.; Yocom, K. M. In *Hydrogels and biodegradable polymers for bioapplications*; Ottenbrite, R. M., Huang, S. J., Park, K., Eds.; American Chemical Society: Washington, DC, 1996; Chapter 10.

10.1021/la011839a CCC: $22.00
Published on Web 08/02/2002

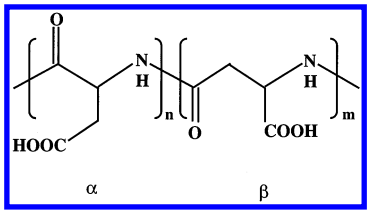

Figure 1. Chemical structure of polyaspartic acid.

ferent pHs. PASP can also be used as a good inhibitor of steel corrosion. Silverman et al.[18] have explored the chelating power of polyaspartic acid on iron, and correlated this with the corrosion inhibition ability of steel by PASP. In the work reported here, the chelating chemistry of PASP with calcium may also affect the calcite dissolution mechanism.

Dissolution of calcium salts occurs by several different chemical, interfacial, and transport mechanisms. In the absence of chelating agents, the dissolution of calcite at low pHs (<4) has been characterized to be mainly mass transfer limited in a variety of acidic media ranging from HCl to pseudo-seawater.[5−8] At high pH (>7), the dissolution of calcite has been shown to depend on both the mass transfer of the reactants and products to the solid surface and the kinetics of the heterogeneous reactions on the calcite surface.[5,6,8] In the presence of strong chelating agents such as EDTA, the rate of dissolution is influenced by the kinetics of interfacial chelation reaction and varies considerably with pH. A surface complexation mechanism was used to describe the rate of calcite dissolution over the pH range of 4−12.[13]

As for other calcium salts, in the absence of chelating agents, the dissolution of a mixture film of brushite and hydroxyapatite in turbulent flows and at pHs ranging from 2.85 to 10 is controlled both by the kinetics of the interfacial dissolution and by mass transfer.[19] In the presence of sodium citrate, a weak sequestrant, the dissolution rate of hydroxyapatite at a neutral pH is inhibited by low concentration of sodium citrate and enhanced at higher concentration.[11] Arbel et al.[12] attributed this to the adsorption and complexation of citrate ions on the crystal surface.

When compared to the agents mentioned above, PASP, as a polymeric chelating agent, has its own unique chemical, interfacial, and transport characteristics in dissolving calcite. The effect of PASP chelation chemistry on the dissolution of calcite is one such characteristic that can be used to elucidate how reaction chemistry and surface interactions play a role in dissolving calcite.

This study presents the results of PASP chelation chemistry and batch dissolution of calcite at four initial pHs (3.5, 5.0, 7, and 10) in the presence and absence of PASP. Special attention is paid to both the effect of chelation chemistry of PASP and interfacial interactions on the dissolution of calcite.

2. Experimental Section

2.1. Materials. Sodium polyaspartate (40 wt % solution, pH 8−9.5, CAS No. 34345-47-6) with a molecular weight of 10 000 was obtained from Donlar Corporation, calcium standard (0.1 M) was from Fisher Scientific, and calcium carbonate solid powder (purity better than 99%) was from Sigma Ultra. Other chemicals were of analytical grade, and were used without further purification. Deionized water was used in all experiments.

(18) Silverman, D. C.; Kalota, D. J.; Stover, F. S. *Corrosion* **1995**, *51*, 818−825.

(19) Littlejohn, F.; Grant, C. S.; Saez, A. E. *Ind. Eng. Chem. Res.* **2000**, *39*, 933−942.

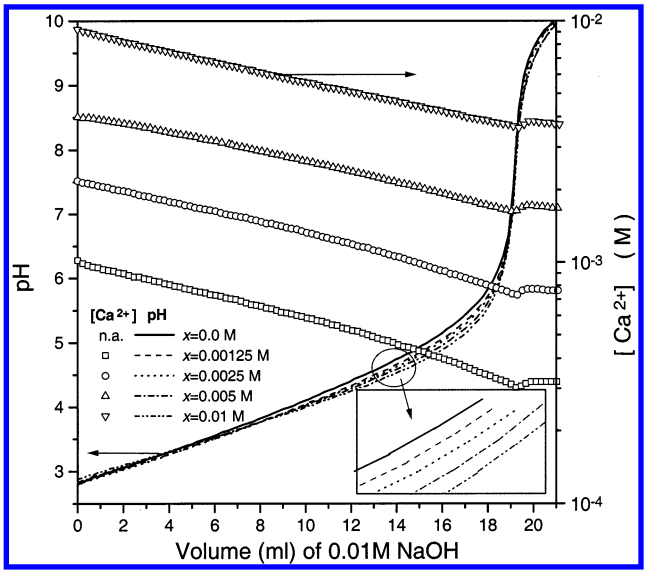

Figure 2. pH (left axis) and free calcium concentration ([Ca^{2+}], right axis) during titration against PASP solutions. PASP solutions consist of (0.01 mequiv sodium polyaspartate + 0.01 M HCl + *x* M $CaCl_2$) at ion strength of 0.2 M. n.a. = not available; *x* denotes the concentration of $CaCl_2$.

2.2. Titration Experiments. The titrations of polyaspartic acid were performed manually under continuous stirring and by use of a 0.01 M NaOH/0.19 M NaCl titrant, and monitored by a pH/ATC electrode (Model 300731.1, Denver Instrument Company) and a calcium ISE electrode (Model 97-20, Orion Research Inc.). Preliminary electrode calibrations with standard buffers (pH 4, 7, and 10) or standard calcium solutions were performed, and the titrant was standardized using 0.01 M primary standard-grade potassium hydrogen phthalate. The following titrations were performed with data taken every 0.2 mL:

(1) 0.01 Meq sodium polyaspartate + 0.01 M HCl to determine the dissociation equilibrium constants (p*K* values) of polyaspartic acid

(2) 0.01 Meq sodium polyaspartate + 0.01 M HCl + 0.001 25, 0.0025, 0.005, or 0.01 M $CaCl_2$ to assess calcium−polyaspartate complexation

The initial volume of each titration was 20 mL. All solutions were adjusted to 0.2 M ion strength by addition of NaCl.

2.3. Batch Dissolution Experiments. Batch dissolution experiments were conducted at room temperature (25 °C) in a 150 mL beaker containing 100 mL of solution. All solutions containing 0.08 M KCl and *x* ppm sodium polyaspartate (*x* ranging from 0 to 2000 ppm) were then adjusted to the desired pH values using 0.01 M HCl, 0.01 M NaOH, or 0.2 M acetic acid buffer. Magnetic stirrers were kept at a constant speed for all runs in order to mix the solution and ensure a uniform aqueous suspension of calcium carbonate. After addition of 1.0 g L^{-1} calcium carbonate powder, the free calcium concentration and pH were determined with the calcium ISE electrode and the pH/ATC electrode. During the run, samples (2 mL each, about 10 samples for a 30 min run) were withdrawn and filtered quickly (less than 10 s) using 0.45 μm Acrodisc 3CR PTFE filters (Gelman Sciences). The total calcium concentration in the samples was measured using a Perkin-Elmer Model AA-100 atomic adsorption spectrophotometer.

3. Results and Discussion

3.1. Chelation Chemistry of Polyaspartic Acid. The titration curve of polyaspartic acid in either the presence or absence of $CaCl_2$, shown in Figure 2, is used to calculate the dissociation constants and calcium-binding constants. The curve was established by titrating a 0.01 mequiv sodium polyaspartate solution containing 0.01 M HCl. It was found that the polyaspartic acid underwent a gradual deprotonation at low pH and reached full deprotonation

Table 1. Dissociation Constants and Calcium Binding Constants of Polyaspartic Acid

	log $K_{A,1}$	log $K_{A,2}$	log $K_{A,3}$	log $K_{A,4}$	log $K_{B,1}$	log $K_{B,2}$	log $K_{B,3}$
this work	5.17	4.09	3.60	2.27	3.02	2.55	2.16
	5.30[a]	4.22[a]	3.72[a]	2.40[a]	3.52[a]	3.05[a]	2.66[a]
ref 18	5.4	4.3	3.60	2.2			

[a] The data are true equilibrium constants, by assuming that the activity coefficients of different deprotonated polyaspartic acid species have the same values as those of calcium−polyaspartate complexes.

at pH 7. This is evidenced by the rapid rise in pH and the slower decrease in free calcium concentrations after pH 7 with the further addition of NaOH. The presence of $CaCl_2$ causes a decrease in pH, and the higher the concentration of $CaCl_2$ in the solution, the lower the pH after a specific addition of NaOH. This effect is more apparent in the range of pH 4−6. Therefore, the presence of $CaCl_2$ increases the required amount of titrant for a given pH, which indicates the binding of calcium with polyaspartate ion.

Sodium polyaspartate with a molecular weight of 10 000 consists of approximately 72 aspartyl residues (both α and β structures, as shown in Figure 1). Each residue may undergo protonation, deprotonation, and calcium-complexation steps in solution. The direct calculation of dissociation constants and calcium-binding constants is difficult. We developed a model to describe the chelating chemistry of polyaspartic acid. Two assumptions were made: (1) the polyaspatic acid is modeled as a molecule having four distinct acid moieties (four pK values), and (2) the equivalent molecular weight of this polyaspartic acid molecule is $4 \times 137 = 548$ (the molecular mass of four aspartyl residues from an actual polyaspartic acid molecule). These two assumptions equivalently mean that an actual polyaspartic acid molecule having 72 repeat units can be modeled as 18 independent hypothetical polyaspartic acid molecules (denoted as H_4L) and each hypothetical molecule has four independent hydrogen protons. Thus, the protonation of this hypothetical molecule involves four distinct reactions:

$$H^+ + L^{4-} = HL^{3-} \quad (1)$$

$$H^+ + H_{n-1}L^{n-5} = H_nL^{n-4} (n = 2, 3, 4) \quad (2)$$

The reactions governing the binding of free calcium with polyaspartate ion can be written as

$$Ca^{2+} + L^{4-} = CaL^{2-} \quad (3)$$

$$Ca^{2+} + H_mL^{m-4} = CaH_mL^{m-2} (m = 1, 2, 3) \quad (4)$$

The concentration based reaction equilibrium constants for eqs 1−4 can be expressed as

$$K_{A,1} = [HL^{3-}]/[H^+][L^{4-}] \quad (5)$$

$$K_{A,n} = [H_nL^{n-4}]/[H^+][H_{n-1}L^{n-5}] (n = 2, 3, 4) \quad (6)$$

$$K_{B,1} = [CaL^{2-}]/[Ca^{2+}][L^{4-}] \quad (7)$$

$$K_{B,m+1} = [CaH_mL^{m-2}]/[Ca^{2+}][H_mL^{m-4}] (m = 1, 2, 3) \quad (8)$$

Since the ion strength of the solution during titration was kept constant at 0.2 M, the correction terms arising from the ion activity coefficients (which are dependent only on ion strength of the solution) become constant for the true equilibrium constants, so that eqs 5−8 can be directly used in a model. Together with the three material balances for polyaspartate ion, total hydrogen, and total calcium, there are a total of $(n + m + 3)$ equations and $(n + m + 3)$ unknown concentrations for all species in the solution. The calculated H^+ concentration (or pH) as well as the concentrations of other species can be solved from these equations. The pH was calculated from the following two equations:

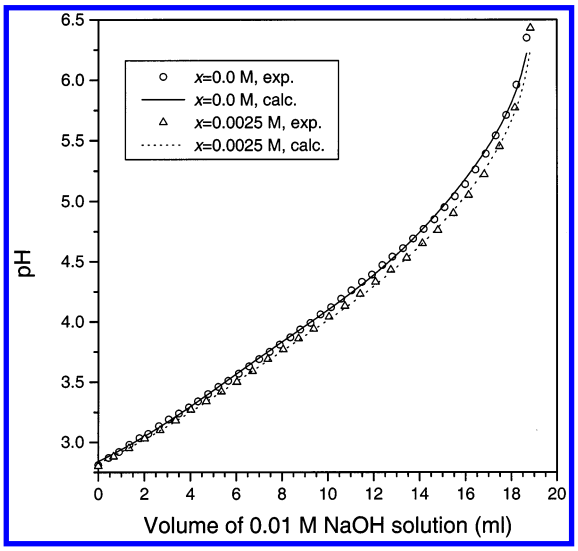

Figure 3. Titration curves between model calculations and experiments for PASP solutions consisting of (0.01 mequiv sodium polyaspartate + 0.01 M HCl + x M $CaCl_2$) at ion strength of 0.2 M. x denotes the concentration of $CaCl_2$.

$$pH = -\log [H^+] - \log \gamma_{[H]} \quad (9)$$

$$\log \gamma_{[H]} = -0.51Z^2\{I^{0.5}/(1 + I^{0.5}) - 0.3I\} \quad (10)$$

where γ is the activity coefficient, Z is the charge of an ion, and I is the ion strength of the solution. Equation 10 is the Davies modification for the Debye−Hückel equation.[20] The sum of square deviation between calculated pH and experimental pH data was used as the objective function and minimized in optimizing the K_A and K_B values with the simplex method.

The m value in the model was allowed to vary from 1 to 3. However, $m = 3$ (CaH_3L^+ as well as CaL^{2-}, $CaHL^-$, and CaH_2L^0 existing in the solution) or $m = 1$ does not accurately represent the experimental titration curves. The best fit to the experimental titration curves was found to have m equal to 2. In this case, the stable calcium ligand species in aqueous solution would be CaL^{2-}, $CaHL^-$, and CaH_2L^0, and the root-mean-square deviation between calculated and experimental pHs is 0.02 pH unit. Table 1 shows the calculated log K_A and log K_B values, while Figure 3 indicates the comparison between the calculated and experimental titration results using these values. Silverman et al.[18] has also reported the dissociation constants for polyaspartic acid (having a different source

(20) Davies, C. W. *Ion Association*; Butterworth: London, 1962.

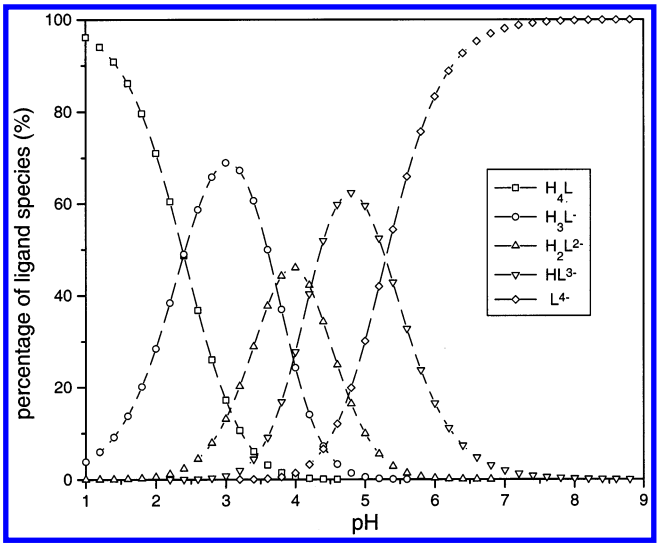

Figure 4. Percentage of polyaspartic acid species as a function of pH in 0.01 mequiv PASP solution with an ion strength of 0.2 M. The data were obtained by using the correlated dissociation constants in Table 1. L is the hypothetical molecule that consists of four aspartyl residues from a real PASP molecule.

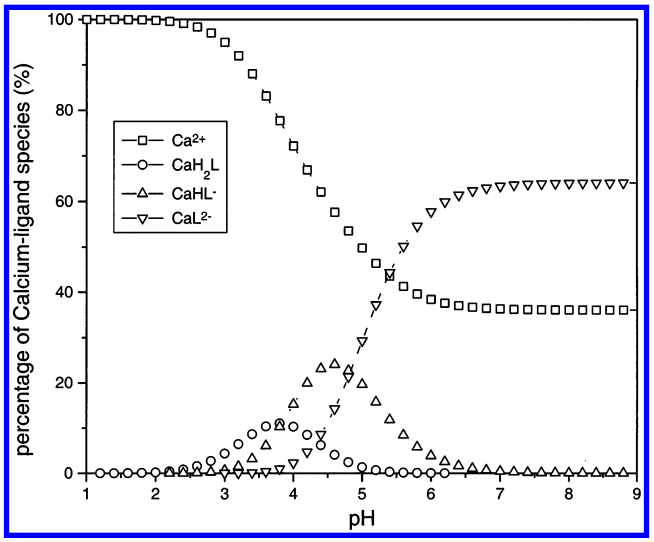

Figure 5. Percentage of calcium−polyaspartate complexation species as function of pH in a solution containing 0.01 mequiv PASP and 0.001 25 M $CaCl_2$. L has the same meaning as in Figure 4.

from ours) when they explored the corrosion inhibition of steel. Their correlated log K_A values, as also shown in Table 1, are consistent with those in this study. This chelation chemistry model provides an excellent foundation for the development of a representative kinetic model for the dissolution of calcite in PASP solutions.

With these K_A and K_B values in hand, the speciation diagram in either the absence or presence of calcium can be generated. Figure 4 shows the speciation plot of polyaspartic acid in the absence of calcium. Figure 5 provides an example of the speciation diagram of calcium−polyaspartate complexes at a total calcium concentration of 0.001 25 M and a total ligand concentration of 0.01 mequiv. The speciation diagrams will enable us to predict the dominant deprotonated ligand species and calcium−PASP complexes at specific pH values. Since H^+, water, and different deprotonated PASP species can all react with calcite on the surface, the dominant species in the solution defines the dissolution mechanism. Therefore, the K_A and K_B values (or the speciation diagrams) are

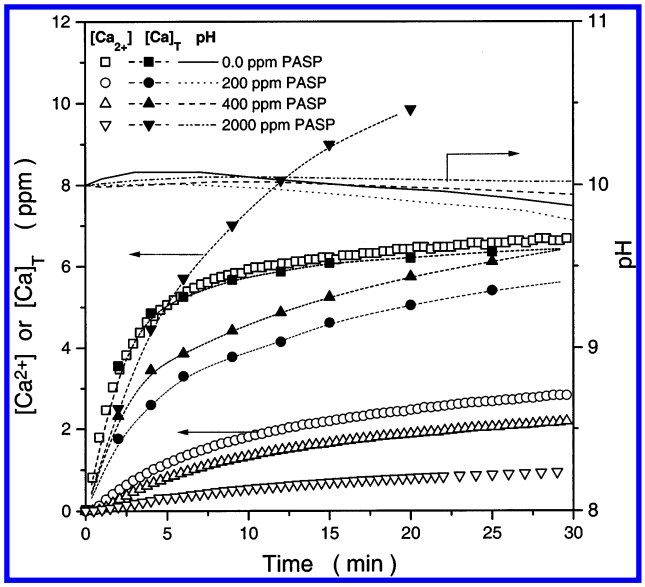

Figure 6. Effect of PASP concentration on free calcium concentration ($[Ca^{2+}]$, left axis), total calcium concentration ($[Ca]_T$, left axis), and pH change (right axis) during dissolution of calcium carbonate powder (1.0 g L^{-1} $CaCO_3$ + 0.08 M KCl) at initial pH 10.

very important for understanding the calcite dissolution in a PASP solution.

3.2. Batch Dissolution of Calcite Powder. *3.2.1. Dissolution in Alkaline PASP Solutions.* The dissolution behavior of calcite in the presence of PASP at initial pH 10 and initial pH 7 is studied using batch dissolution experiments. This pH range was selected to eliminate the effect of hydrogen ion attack and focuses on the L^{4-} form of the agent. Because PASP can become fully deprotonated at about pH 7 (see Figures 2 and 4), the complications associated with multiple ionic species and dissociation reactions are negligible, and the calcium−PASP complex is also only in the form of CaL^{2-}. Figure 6 shows the total calcium concentration in the supernatant, the free calcium concentration, and pH as a function of time during calcite dissolution at initial pH 10. The concentration of sodium polyaspartate in solution ranges from 0 to 2000 ppm. As can be seen, increasing the concentration of sodium polyaspartate always decreases the free calcium concentration ($[Ca^{2+}]$, measured by calcium ISE electrode). In the presence of PASP, the total calcium concentration ($[Ca]_T$, includes $[Ca^{2+}]$ and all other calcium-containing species, measured by atomic absorption), is always larger than $[Ca^{2+}]$, indicating the presence of calcium−PASP complexes in the solution. An interesting point is the presence of an initial lag time for the free calcium concentration profile (within this lag time, the free calcium concentration is zero). The higher the initial PASP concentration, the longer the lag time. However, in comparison to the case of calcite powder dissolved in pure water (0.0 ppm PASP), the presence of PASP (2000 ppm) causes lower dissolution rates at the beginning period of the run (first several minutes). After this period, the dissolution rate in the presence of PASP becomes larger than that in pure water. For the pH profile, no significant pH changes are found during all the runs, which implies that the carbonate ion (CO_3^{2-}) released from the surface exists in the solution in a nearly equimolar mixture of CO_3^{2-} and HCO_3^- (since the pK value for HCO_3^- is about 10).

The dissolution behavior of calcium carbonate powder at initial pH 7 is also determined and shown in Figure 7. Similar results with the case at initial pH 10 are obtained.

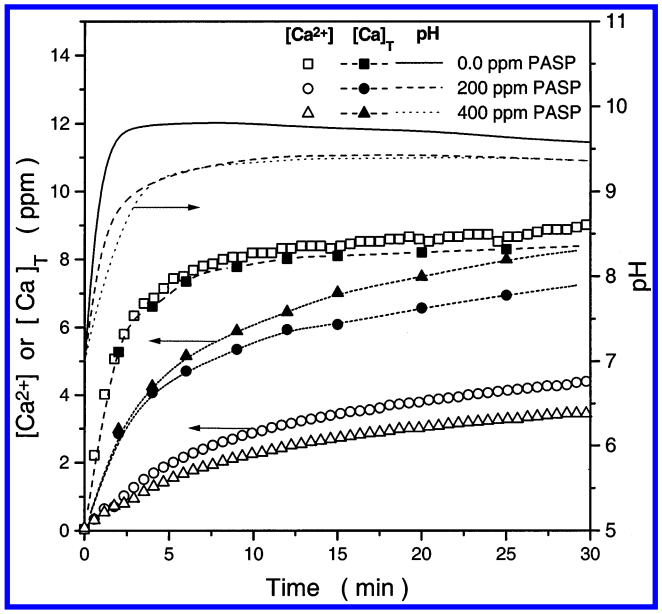

Figure 7. Effect of PASP concentration on free calcium concentration ($[Ca^{2+}]$, left axis), total calcium concentration ($[Ca]_T$, left axis), and pH change (right axis) during dissolution of calcium carbonate powder (1.0 g L^{-1} $CaCO_3$ + 0.08 M KCl) at initial pH 7.

The main difference is that no lag time for the free calcium profile is found in this case. This is because H^+ (about 10^{-7} M in concentration) contributes to some extent to the calcite dissolution at the first 1−2 min of the runs (evidenced from the rapid pH rise in this period of time). Besides the small contribution from H^+, the dissolution of calcite at initial pH 7 keeps the same mechanism as the case at initial pH 10.

It was clearly shown from Figures 6 and 7 that the dissolution behavior in the presence of PASP at alkaline pHs is quite different from the cases in the absence of PASP, suggesting the strong possibility of PASP replacing water to react with calcium carbonate on the surface. Detailed studies of the dissolution mechanism of calcite in pure water[8,21] indicate that water adsorbs onto the calcite surface and is subsequently dissociated. The surface reaction is initiated by the dissociated hydrogen ions on the surface and involves desorption of calcium and carbonate products. When PASP is present in the solution, besides the water reaction, PASP may also be adsorbed onto the surface and react with calcium on the surface. The mechanism for the calcite dissolution at high pHs (>7), contributed from the chelating reaction, can be written as

$$L^{4-} = L^{4-}{}_{(ads)} \quad (11)$$

$$L^{4-}{}_{(ads)} + CaCO_{3\,(lattice)} = CaL^{2-}{}_{(ads)} + CO_3^{2-}{}_{(ads)} \quad (12)$$

$$CaL^{2-}{}_{(ads)} = CaL^{2-}{}_{(i)} \quad (13)$$

$$CO_3^{2-}{}_{(ads)} = CO_3^{2-}{}_{(i)} \quad (14)$$

where (ads) and (i) indicate species adsorbed on the surface and located at the solid−liquid interface, respectively. Fredd and Fogler[13] have proposed a similar mechanism for the dissolution of calcite in EDTA solutions. Following their derivation, the overall dissolution rate of calcite in PASP solution can be represented as

$$r_T = r_L + r_w \quad (15)$$

where r_T, r_L, and r_w are the overall dissolution rate, the reaction rate of PASP, and the reaction rate of water, respectively. Assuming the reaction of the desociated H^+ with the calcite surface is the rate-limiting step for the water reaction, r_w can be expressed as[8,22]

$$r_w = k_{rw}\theta_c\theta_a(1 - [Ca^{2+}]_{(i)}[CO_3^{2-}]_{(i)}/K_{sp}) \quad (16)$$

where k_{rw} is the surface reaction rate constant of water and K_{sp} (=2.2 × 10^{-8} mol^2 dm^{-2}) is the concentration-based solubility product of calcium carbonate. By the same reasoning, assuming the reaction of the adsorbed PASP with the calcite surface (eq 12) is the rate-limiting step for the chelant reaction, following a similar derivation as for r_w, r_L can be derived as

$$r_L = k_L K_L \theta_c \theta_a([L^{4-}]_{(i)} - [CaL^{2-}]_{(i)}[CO_3^{2-}]_{(i)}/K_{eq}) \quad (17)$$

where k_L is the surface reaction rate constant of PASP and K_{eq} is the concentration-based equilibrium constant of eq 12; $K_{eq} = K_{sp}K_{B,1} = 2.3 \times 10^{-5}$ mol dm^{-1}. θ_c and θ_a are the fractions of cations and anions, respectively, which are occupied by absorbed species on the calcite surface

$$\theta_c = 1/(1 + K_{CaL}[CaL^{2-}]_{(i)} + K_{Ca}[Ca^{2+}]_{(i)} + K_H[H^+]_{(i)}) \quad (18)$$

$$\theta_a = 1/(1 + K_L[L^{4-}]_{(i)} + K_{CO_3}[CO_3^{2-}]_{(i)} + K_{OH}[OH^-]_{(i)}) \quad (19)$$

where K_j ($j = Ca^{2+}$, CaL^{2-}, H^+, L^{4-}, CO_3^{2-}, or OH^-) are the Langmuirian adsorption equilibrium constants. The HCO_3^- species does not enter into the expression of θ_a, since between the two carbonate species only CO_3^{2-} is found to be in significant concentration on the calcite surface in alkaline solutions.[23]

In the calculation, it is assumed that mass transfer has little influence on the dissolution so that the concentration of each species at interface is equal to that in the bulk solution. This assumption is valid for calcite dissolution in pure water[6] and EDTA solutions[13] at high pHs and high flow rates of the solution (or stirring speed). In addition, since the H^+ concentration is very low at high pH, the term $K_H[H^+]_{(i)}$ in eq 18 can be neglected. Some adsorption equilibrium constants in calcite systems (K_{CO_3} = 3 × 10^4 dm^3 mol^{-1}, K_{OH} = 700 dm^3 mol^{-1}, K_{Ca} = 1000 dm^3 mol^{-1}) are obtained from literature.[22] The remaining parameters in eqs 15−17, k_w, k_L, K_L, and K_{CaL}, are determined by fitting to the experimental data, and the resulting values are shown in Table 2. The calculated dissolution rate from eq 15 is given in Figure 8 and compared with the experimental data. The experimental dissolution rates are the derivatives of $[Ca]_T$ (shown in Figure 6) with respect to time by the use of spline function fitting and smoothing. Reasonable agreement between

Table 2. Model Parameters for Calcite Dissolution in PASP Solutions (pH 10)

k_{rw} (mol min^{-1})	k_L (mol min^{-1})	K_L (dm^3 mol^{-1})	K_{CaL} (dm^3 mol^{-1})
7.8 × 10^{-5}	4.2 × 10^{-5}	4.2 × 10^3	6.3 × 10^3

(21) Brown, C. A.; Compton, R. G.; Narramore, C. A. *J. Colloid Interface Sci.* **1993**, *160*, 372−379.

(22) Compton, R. G.; Brown, C. A. *J. Colloid Interface Sci.* **1994**, *165*, 445−449.

(23) Thompson, D. W.; Pownall, P. G. *J. Colloid Interface Sci.* **1989**, *131*, 74−82.

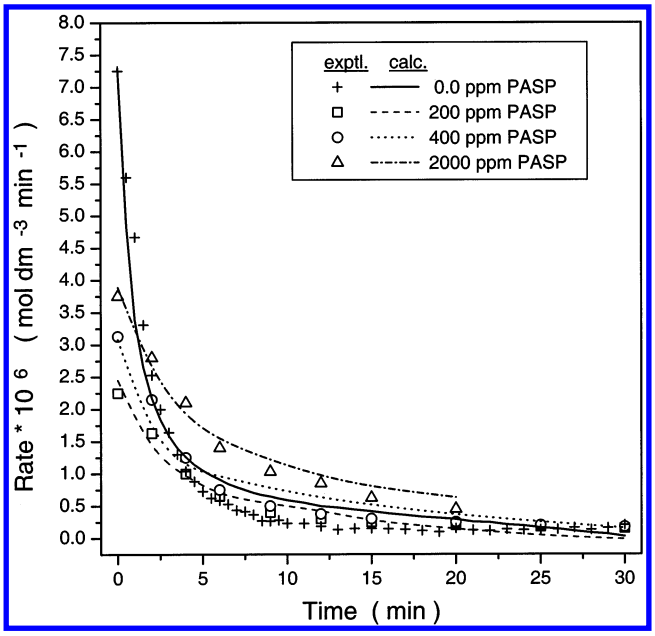

Figure 8. Comparison of experimental and calculated dissolution rates of calcium carbonate powder (1.0 g L^{-1} $CaCO_3$ + 0.08 M KCl) at initial pH 10 and different PASP concentrations.

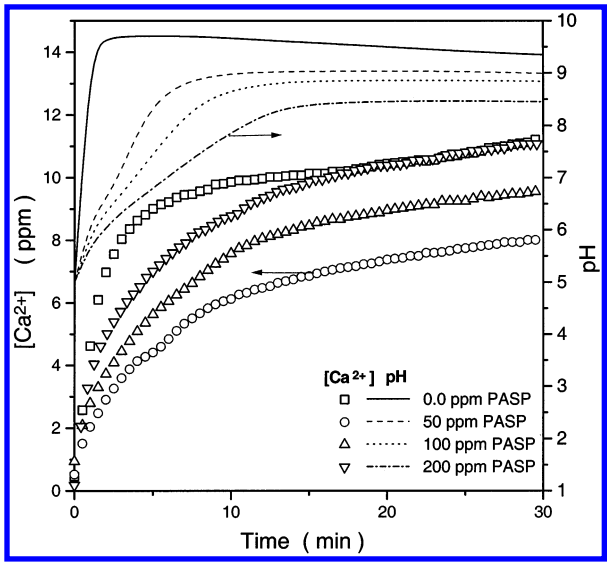

Figure 9. Effect of PASP concentration on free calcium concentration ($[Ca^{2+}]$, left axis) and pH change (right axis) during dissolution of calcium carbonate powder (1.0 g L^{-1} $CaCO_3$ + 0.08 M KCl) at initial pH 5.

the calculated and experimental dissolution data is obtained. In addition, calculations show that the water reaction with calcite is inhibited when PASP is present in the solution. Otherwise, the model will always predict a higher dissolution rate in PASP solution than that in pure water in the whole time range studied, which contradicts the experimental results. A possible explanation is that PASP on the calcite interface inhibits the dissociation of water, causing the absence of dissociated hydrogen protons to initiate the water reaction. Another interesting point is that the adsorption constant for the calcium−PASP complex is larger than that for the free PASP (see Table 2). Fredd and Fogler[13] have studied the calcite dissolution in EDTA solution and revealed a lower adsorption constant for the complex than for the free chelating agent. This indicates one of the differences in calcite dissolution mechanisms between PASP and EDTA agents.

3.2.2. Dissolution in Acidic PASP Solutions. When pH is lowered to 5, the chelation chemistry of PASP shows that the species dominating in the solution takes the forms of HL^{3-} (≈50%) and L^{4-} (≈40%), and the complexes are in the form of $CaHL^{-}$ and CaL^{2-} (see Figures 4 and 5). Figure 9 gives the dissolution behavior of calcite in pure water and PASP solutions at initial pH 5. Figure 10 shows results in 0.2 M acetic acid (HAc) buffered solution of pH 5.0. For the former case, since only the initial pH is fixed, the total hydrogen or acidity (including free H^+ and bonded hydrogen with PASP) in PASP solutions increases with increasing PASP concentration. For the latter case, 0.2 M HAc buffer is used to keep the total hydrogen (including free H^+ and bonded hydrogen with PASP and HAc) in excess and constant for all runs in Figure 10, and the pH of solution also changes very little during a run. It is shown in Figure 9 that increasing PASP concentration increases the free calcium concentration and also the total calcium concentration (not measured, but it can be easily calculated using the chelation chemistry model developed in section 3.1). However, the free calcium concentration in the presence of PASP is lower than that in pure water (0.0 ppm PASP). This free calcium profile is very similar to the total calcium profile at initial pH 10 (see Figures 6

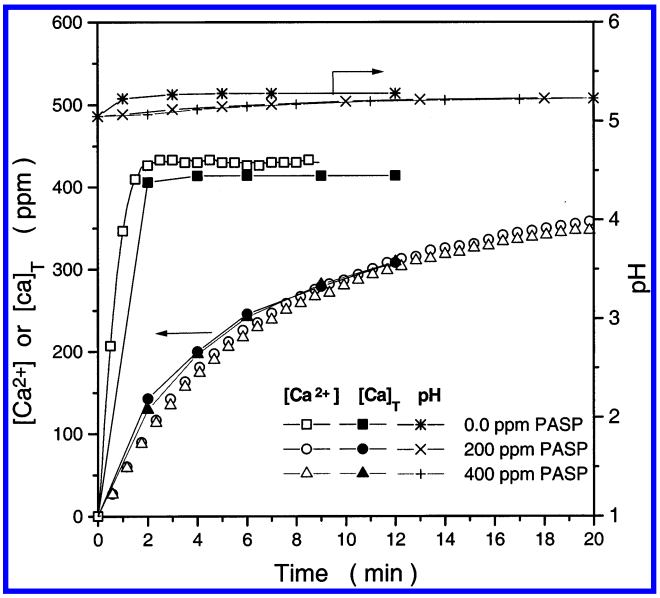

Figure 10. Effect of PASP concentration on free calcium concentration ($[Ca^{2+}]$, left axis), total calcium concentration ($[Ca]_T$, left axis), and pH change (right axis) during dissolution of calcium carbonate powder (1.0 g L^{-1} $CaCO_3$ + 0.08 M KCl) in 0.2 M acetic acid buffer of pH 5.

and 9). All these indicate that the calcite dissolution in the presence of PASP may be affected by both H^+ attack and PASP-chelating attack.

When the solution is buffered at pH 5, as shown in Figure 10, calcite is completely dissolved in 2 min in pure water, while only three-fourths of the calcite gets dissolved in 20 min in the presence of PASP. PASP concentration has little influence on the calcite dissolution, and the total calcium concentration in the presence of PASP is only slightly higher than the free calcium concentration. Since the total hydrogen is kept in excess and constant for all runs in this case, the calcite dissolution rate is mainly determined by the total acidity in the solution and the available reaction sites on calcite surface for acidic species (including H^+, HAc, and HL^{3-}). The L^{4-} chelation reaction itself contributes little to the dissolution rate at pH 5, but the adsorption of PASP on the calcite surface greatly decreases the fraction of acidic species occupying the

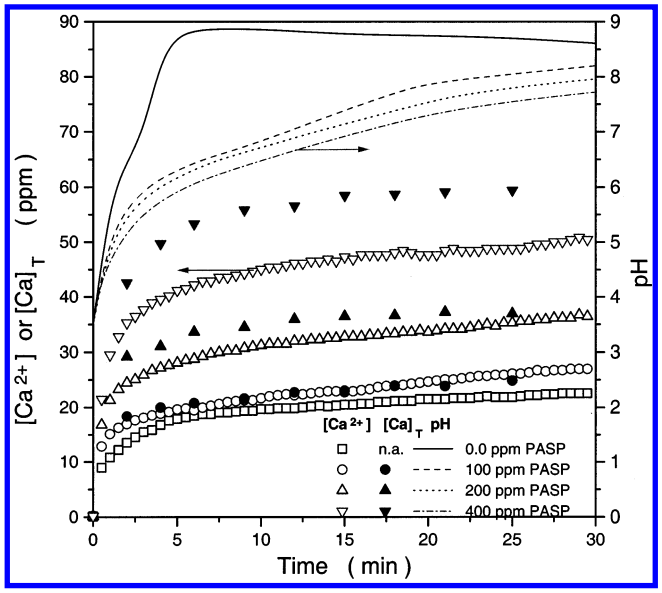

Figure 11. Effect of PASP concentration on free calcium concentration ($[Ca^{2+}]$, left axis), total calcium concentration ($[Ca]_T$, left axis), and pH change (right axis) during dissolution of calcium carbonate powder (1.0 g L^{-1} $CaCO_3$ + 0.08 M KCl) at initial pH 3.5. n.a. = not available.

reaction sites. The dissolution results with a buffer are consistent with experiments in the absence of a buffer.

When the initial pH was changed to 3.5, the dominating PASP species are H_3L^- (≈55%) and H_2L^{2-} (≈35%) (see Figure 4). The chelating ability of H_2L^{2-} with calcium also becomes much weaker than that of the fully deprotoated form. In this case, both free calcium and the total calcium concentrations in the presence of PASP, as shown in Figure 11, increase with increasing PASP concentration. The dissolution rate of calcite in the presence of PASP is also larger than that in pure water, indicating that the calcite dissolution was mainly determined by the total acidity (including H^+, H_2L^{2-}, and H_3L^-). The adsorption and chelating reactions of PASP on the calcite surface still occur, but they become a secondary factor, since only about 30% of the PASP active groups are deprotonated. Hence, the lower the pH, the less the PASP chelating chemistry affects the dissolution behavior of calcite. In this case, PASP becomes a mild provider or carrier of H^+ ions.

In fact, at low pH, the rate of dissolution is influenced by a combination of acidic species attacks (including H^+ and H_nL^{n-4}, $n = 1, 2, 3, 4$) and chelant attacks (H_nL^{n-4} and L^{4-}, $n = 1, 2$). The mechanism of calcite dissolution can be written as

$$H^+_{(ads)} + CaCO_{3\,(lattice)} = Ca^{2+}_{(ads)} + HCO_3^-{}_{(ads)} \quad (20)$$

$$H_nL^{n-4}_{(ads)} + CaCO_{3\,(lattice)} = Ca^{2+}_{(ads)} + H_{n-1}L^{n-5}_{(ads)} + HCO_3^{2-}{}_{(ads)} \quad (21a)$$

$$H_nL^{n-4}_{(ads)} + CaCO_{3\,(lattice)} = CaH_nL^{n-2}_{(ads)} + CO_3^{2-}{}_{(ads)} \quad (21b)$$

$$L^{4-}_{(ads)} + CaCO_{3\,(lattice)} = CaL^{2-}_{(ads)} + CO_3^{2-}{}_{(ads)} \quad (22)$$

where only the limiting-step reactions are listed. Equations 20 and 21a belong to the acidic species attacks, while eqs 21b and 22 are the chelant attacks. Therefore, the corresponding total dissolution rate should be expressed as

$$r_T = r_H + \sum[y_n r^a{}_{H_nL} + (1 - y_n) r^b{}_{H_nL}] + r_L \quad (23)$$

$$r_H = k_H K_H \theta_c \theta_a [H^+]_{(i)} \quad (24)$$

where y_n is the molar fraction of H_nL^{n-4} species that undergoes the reaction in eq 21a. A first-order reaction of H^+ with calcite is assumed to express r_H. Since the reaction of H^+ with calcite is nearly irreversible, the effect of the reverse reaction of H^+ with calcite on r_H is neglected. By the same reasoning, an expression similar to that for r_H can be derived for $r^a{}_{H_nL}$, where $k_H K_H$ in eq 24 should be replaced with $k^a{}_{H_nL} K_{H_nL}$ and $[H^+]_{(i)}$ with $[H_nL]_{(i)}$. $r^b{}_{H_nL}$ is the rate for chelating reaction between calcite and deprotonated PASP ligand (H_nL^{n-4}, $n = 1, 2$), and takes the same expression as that for r_L if the appropriate surface reaction rate and adsorption constants ($k^b{}_{H_nL}$ and K_{H_nL}) for each deprotonated ligand are used.

Since the calcite dissolution at low pH usually involves two major deprotonated PASP species at one time, more than nine model parameters need to be regressed from the experimental data. In addition, mass transfer will also become significant at low pH until it becomes the limiting step.[5,8,13] However, in the batch dissolution experiments, the mass transfer is not well characterized and the sharp pH change (see Figures 9 and 11) during the runs also causes difficulty in calculation. Therefore, the batch dissolution experimental data at low pHs are qualitative rather than quantitative. More accurate and mass transfer controlled experimental methods, such as a rotating disk experiment,[7,24] will be incorporated for further study.

4. Conclusions

The potentiometric titration of PASP and the batch dissolution of calcite in the presence of PASP at initial pHs ranging from 3.5 to 10 are investigated in this study. The titration reveals that the PASP undergoes a successive deprotonation until pH 7 and can be modeled successfully as a species of four distinct acidic moieties. The dissociation constants (pK values) for these moieties are 2.27, 3.60, 4.09, and 5.17. The complexation and speciation of PASP with calcium calculated by the chelation chemistry model show different binding of PASP with calcium at different pHs, which should account for the different dissolution behavior of calcite. In the presence of PASP, the dissolution of calcite at high pH (>7) is quite different from that in pure water, and can be described by a surface adsorption and complexation mechanism.

At low pHs (≤5), the dissolution rate of calcite in the presence of PASP increases with increasing PASP concentration and total acidity in the solution. Both acidic species attacks (including H^+ and H_nL^{4-n}, $n = 1, 2, 3, 4$) and chelant attacks (including H_nL^{4-n} and L^{4-}, $n = 1, 2$) become the dominating reactions on the calcite surfaces. Calcite dissolution in acidic PASP solutions involves multiple surface reactions in addition to mass transfer and represents the most complicated case; this requires more careful theoretical and experimental investigation. For the whole pH range studied here (from 3.5 to 10), the chelation chemistry has a strong influence on the adsorption of PASP and its interfacial interactions that play an important role in calcite dissolution.

(24) Beaudoin, S. P.; Grant, C. S.; Carbonell, R. G. *Ind. Eng. Chem. Res.* **1995**, *34*, 3307−3325.

Acknowledgment. We thank the National Science Foundation for the financial support (Grant CTS-9905152). Thanks to FB Grant for manuscript review and editing. We also greatly appreciate Drs. R. Pietrangelo and G. Fan from Donlar Corporation for their technical input and for providing the sodium polyaspartate. Conversations with L. Yu of NIST are also appreciated.
LA011839A